Simulated phantom images for optimizing wavelet based image processing algorithms in mammography

Yunong Xing[a]
Walter Huda[b]
Andrew Laine[c]
Jian Fan[c]

Departments of Electrical Engineering[a], Radiology[b] and
Computer & Information Sciences[c], University of Florida,
Gainesville, Florida 32610

ABSTRACT

Image processing techniques using wavelet signal analysis have shown some promise in mammography. It is desirable, however, to optimize these algorithms before subjecting them to clinical evaluation. In this study, computer simulated images were used to study the significance of all the parameters available in a multiscale wavelet image processing algorithm designed to enhance mammograms. Computer simulated images had a gaussian-shaped signal in half of the regions of interest and included added random noise. Signal intensity and noise levels were varied to determine the detection threshold contrast-to-noise ratio (CNR). An index of the ratio of output to input contrast to noise ratios was used to optimize a wavelet based image processing algorithm. Computed CNRs were generally found to correlate well with signal detection by human observers in *both* the original and processed images. Use of simulated phantom images enabled the parameters associated with multiscale wavelet based processing techniques to be optimized.

Keywords: Wavelets, image processing, mammography, image quality, signal detection, psychophysics, medical imaging

1. INTRODUCTION

High resolution digital mammography systems are presently undergoing clinical testing and their introduction into routine clinical practice is imminent.[8] Availability of digital mammographic data will stimulate the development of effective digital image processing techniques and workstations for use in mammography.[2] A novel approach to image processing is to utilize the wavelet transform which has shown promise when used to enhance mammograms.[3,4,5] One difficulty encountered is the large number of parameters that the algorithms based on the wavelet transform may have.[1,7] It is, therefore, helpful to develop techniques which permit a systematic evaluation of wavelet image processing algorithms for use in mammography.

In this paper, a computer simulated phantom image was used to mimic features of interest in mammography. The signal intensity was varied to ensure that the results included those at the threshold of visual detection. Use of the phantom permitted the generation of a *quantitative index* of algorithm performance, i.e. the ratio of output to input contrast to noise ratios. This performance index may be validated by measuring signal detection achieved by human observers viewing processed images.

2. METHOD

2.1. Mathematical phantom design

Computer simulated phantoms consisted of a 512^2 image matrix and 8 bits per pixel (= 256 gray levels). The phantom was divided into 25 equal squares (i.e. a 5 x 5 grid) with each square having 100^2 pixels. Twelve squares contained a truncated gaussian shaped signal, with the signal containing squares randomly distributed. The peak signal intensity above the background level was I ($5 \leq I \leq 50$) and the radius of the truncated gaussian signal was 25 pixels. Random gaussian noise, with a standard deviation σ, was obtained using the Matlab software package (The Mathworks Inc., Natick, MA) and was added to each of the 25 squares. The mean noise level was a gray level value of 128.

0-8194-1623-1/94/$6.00

By varying the value of the peak signal intensity, I, and the image noise, σ, the visibility of the gaussian signals could be altered. Phantom images were inspected on the monitor of a SUN workstation under identical display (i.e. selected window and level) and viewing conditions (i.e. luminance and illumination levels). This procedure was adopted to ensure consistency when measuring the *relative* observer detection performance. Fig. 1a shows a typical input phantom image. Figs. 1b, c, and d show the corresponding processed images obtained after the input shown in Fig. 1a was processed using different gain settings of an optimized algorithm (see below).

2.2. Processing algorithms

The algorithm evaluated in this study was based on a Dyadic Transform (DT)[7] which permits a perfect reconstruction of the original image. The inner product of a signal (S) with a wavelet (ϕ) reflects the character of S within the time-frequency region where ϕ is localized. Provided ϕ is spatially localized, two-dimensional features such as shape and orientation will be preserved in transform space and can thus be used to characterize these features through scale space.

A multiresolution representation divides the frequency spectrum of an image x into a low-pass sub-band image y_o^L and a set of band-pass sub-band images y_j^i, i=1, ...L and j=1, ... M, where L and M denote the number of levels and orientations for a representation, respectively. If F_j^i is the equivalent filter for the ith level and jth channel, W_{ij} [x] denotes the operation of filtering x. The sub-band image of an L-level multiresolution decomposition is then given by

$$y_j^i = W_{ij}[x] \qquad (1)$$

The two-dimensional dyadic wavelet transform results in a multiresolution representation which partitions orientations into two bands (i.e. M = 2) corresponding to horizontal and vertical bands.[3,5]

At each level i, the two dimensional wavelet maxima coefficients were determined.[4] Maxima above some threshold value T are multiplied by a gain factor, G, followed by the inverse wavelet transform to generate the processed image. Accordingly, there are three parameters that may be selected for the image processing algorithm: (1) a *single* selected level (i = 1 through i = 8) at which the modifications to the wavelet coefficients are to be performed with i = 1 corresponding to the highest spatial frequencies and i = 8 to the lowest (i.e. the DC cap); (2) the threshold value T above which wavelet coefficients are modified; and (3) the gain factor G by which selected wavelet coefficients (i.e. those corresponding to local maxima and above the threshold value T) are to be multiplied.

2.3. Evaluation parameters

The mean signal contrast, C, in the simulated phantom images was defined by

$$C = \frac{1}{12} \cdot \sum_{j=1}^{j=12} \frac{(S_j - B_j)}{\pi \cdot 25^2} \qquad (2)$$

where S_j was the gross signal count in the jth square where the summation was over the central area containing the gaussian signal (i.e. up to r = 25 pixels) and B_j is the corresponding gross counts in an adjacent square *without* the gaussian signal. The noise, N, in the simulated image was defined as

$$N = \frac{1}{12} \cdot \sum_{j=1}^{j=12} \sigma_{B_j} \quad (3)$$

where σ_{Bj} is the standard deviation in the central region of the jth square which does *not* contain any gaussian signal. These definitions for contrast and noise were used to obtain the input contrast to noise ratio (CNR_i) and the corresponding value of the output contrast to noise ratio (CNR_o) in the processed image. The resultant enhancement factor, EF, is then given by the expression

$$EF = \frac{CNR_o}{CNR_i} \quad (4)$$

Observers viewed the simulated phantom image and indicated the presence of a signal in each squares, with a score of 1/2 permitted for borderline visibility. The imaging performance criterion used was the effective sensitivity, TP', defined by

$$TP' = TP - FP \quad (5)$$

where TP is the number of True Positives and FP is the number of False Positives. Fig. 2 shows the results for a single observer as the CNR was varied which shows how the TP' value increases as CNR increases. We observed that for *all* the data points depicted in Fig. 2, the FP value was always zero.

3. RESULTS AND DISCUSSION

3.1. Decomposition level (i)

Fig. 3 shows how the enhancement factor (EF) varied as a function of decomposition level i for three different values of contrast at the same noise level (N = 40). These results show that there is a significant enhancement for the levels 3 to 6 with the maximum enhancement occurring at level i equal to 4. This pattern was also maintained when the CNR = 0.19 corresponds to a 50% effective sensitivity (TP') as depicted in Fig. 2b). These results suggest that this type of image may be improved provided the wavelet coefficients are modified at the appropriate level(s). The lowest decomposition level (i = 1), corresponds to the highest spatial frequencies. Level i = 1 thus contain mainly noise with little signal energy and enhancement of wavelet coefficients at this level result in EF values markedly lower than 1.0. Selection of the highest decomposition levels, where i = 7 or 8, corresponds to the *lowest* spatial frequencies and result in CNR no improvement. The low spatial frequencies contain little of the signal energy and with no significant enhancement of image noise, the resultant value of EF is 1.0. Level i = 4 produced the highest EF values for this specific input signal, and this i value was selected for use in *all* subsequent experiments.

3.2. Threshold (T)

Figs. 4 and 5 show the effect of the threshold parameter on enhancement. In Fig. 4, the contrast level was altered with the gain parameter fixed at 20, and showed that the enhancement effect falls off above a threshold value that is a function of signal contrast. As expected, when the threshold is still further increased, the enhancement factor falls to 1.0 demonstrating that there are no modifications to the wavelet coefficients and thus no change in the processed image. In Fig. 5, the same pattern of EF variation with threshold T is observed as the noise level was altered. Figs. 4 and 5 also show that as the noise level increases relative to the signal intensity, the uncertainty associated with the computed data points, as depicted by the error bars, increased significantly.

3.3. Gain (G)

Fig. 6a shows how the enhancement factor value increasef with gain parameter, clearly suggesting that the processed image was superior to the original. All of the images were viewed by human observers and the location of signals recorded. The True Positives and False Positives, recorded as a function of the Gain parameter, are depicted for one observer in Figs. 6b and c, respectively. In all cases, images processed with a gain of 1 produced observer performance values which were low (≤ 3) and, as to be expected, the results were similar to those obtained for an original (i.e. unprocessed) image. As the gain increased, so did the True Positive score as depicted in Fig. 6b), indicating that imaging performance improves. However, as seen in Fig. 6c), increasing the gain eventually results in False Positives. The reason for this may be seen by inspection of the images depicted in Fig. 1. At the highest gain value (G = 160 in Fig. 1d), structured noise is introduced by this algorithm which may be expected to result in apparent signals in squares which in fact contain no signal.

4. CONCLUSIONS

1. A computer simulated phantom was developed to characterize and optimize wavelet based image enhancement algorithms.

2. The phantom permitted the computation of an enhancement factor (EF) which measured algorithm performance, where the EF was the ratio of output to input Contrast to Noise ratios.

3. Computed EF values correlated very well with human signal detection performances.

4. Use of a wavelet transform improved the detection of gaussian signals embedded in backgrounds or random noise, even at the lowest threshold of visual detection.

5. ACKNOWLEDGMENTS

The authors wish to thank Drs. Janice C. Honeyman, Edward V. Staab, and Barbara G. Steinbach for their assistance in this research project. Editorial assistance by Linda Pigott is truly appreciated.

This work was sponsored in part by the Whittaker Foundation and the U. S. Army Medical Research and Development Command, Grant No. DAMD17-93-J-3003.

6. REFERENCES

1. Daubechies I. "Ten lectures on wavelets," Society for Industrial and Applied Mathematics, Philadelphia, PA, 1992.

2. Giger ML. "Computer aided diagnosis," Technical Aspects of Breast Imaging, Haus AG, MJ Yaffe (eds), Syllabus published by the Radiological Society of North America (1993 RSNA), Oak Brook, IL, pp. 283-298, 1993.

3. Laine A and Song S "Multiscale wavelet representations for mammographic feature analysis," Proceedings of SPIE: Conference on Mathematical Methods in Medical Imaging, San Diego, CA, July 23-25, 1992.

4. Laine A, Schuler S, Huda W, Honeyman JC and Steinbach BG. "Hexagonal wavelet processing of digital mammography," Proceedings of SPIE Conference on Medical Imaging VII, Newport Beach, SPIE, Vol. 1898, pp. 559-573, 1993.

5. Laine A, Song S, Fan J, Huda W, Honeyman JC, Steinbach BG. "Adaptive multiscale processing for contrast enhancement," Proceedings of the SPIE (San Jose), SPIE, Vol. 1905, pp. 521-532, 1993.

6. Mallat SA. "Theory for multiresolution signal decomposition: the wavelet representation. IEEE Transactions on Pattern Analysis and Machine Intelligence, Vol. 11(7), pp. 674-693, 1989.

7. Mallat S and Zhong S. "Characterization of signals from multiscale edges," IEEE Transactions on Pattern Analysis and Machine Intelligence, Vol. 14(7), 1992.

8. Yaffe M. "Digital mammography," Technical Aspects of Breast Imaging, Haus AG, Yaffe MJ (eds), Syllabus published by the Radiological Society of North America (RSNA), Oak Brook, IL, pp. 271-282, 1993.

L = 4; T = 0.25 Contrast = 7.5

[CNR = 0.25] Noise = 30

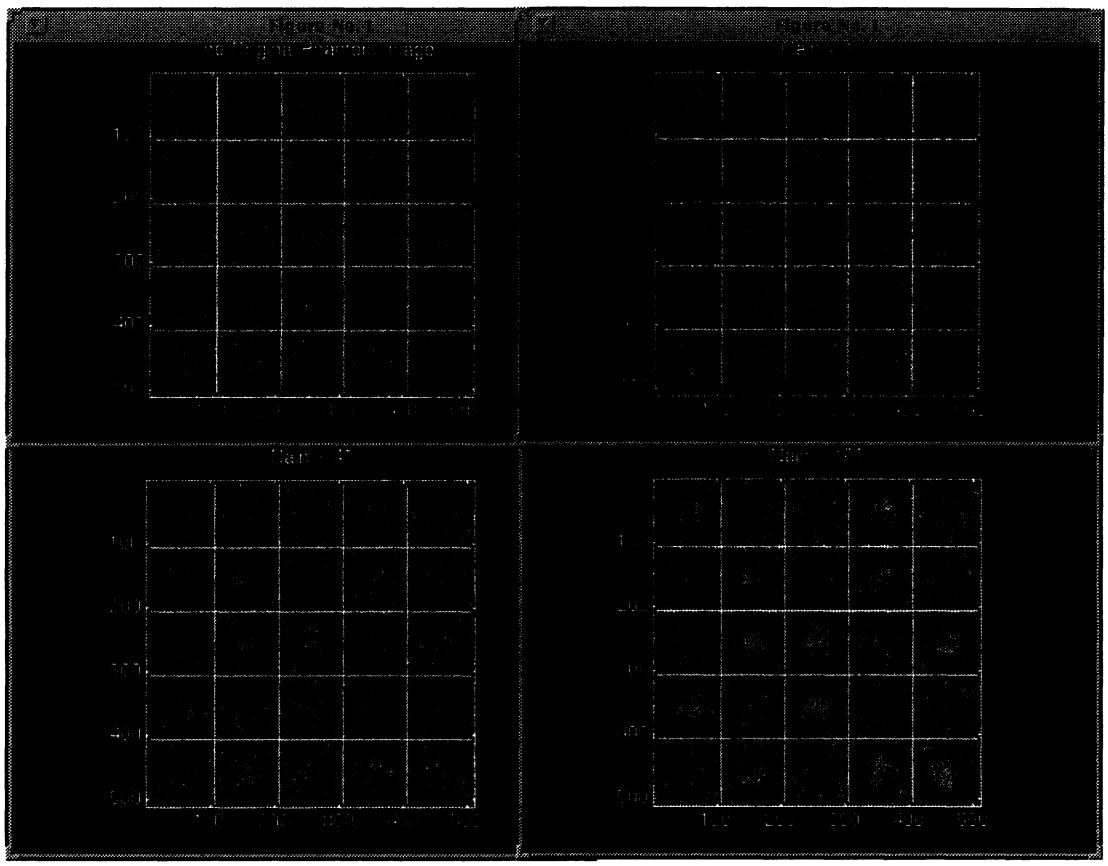

Figure 1

A: Original B: Gain 1 C: Gain 40 D: Gain 160

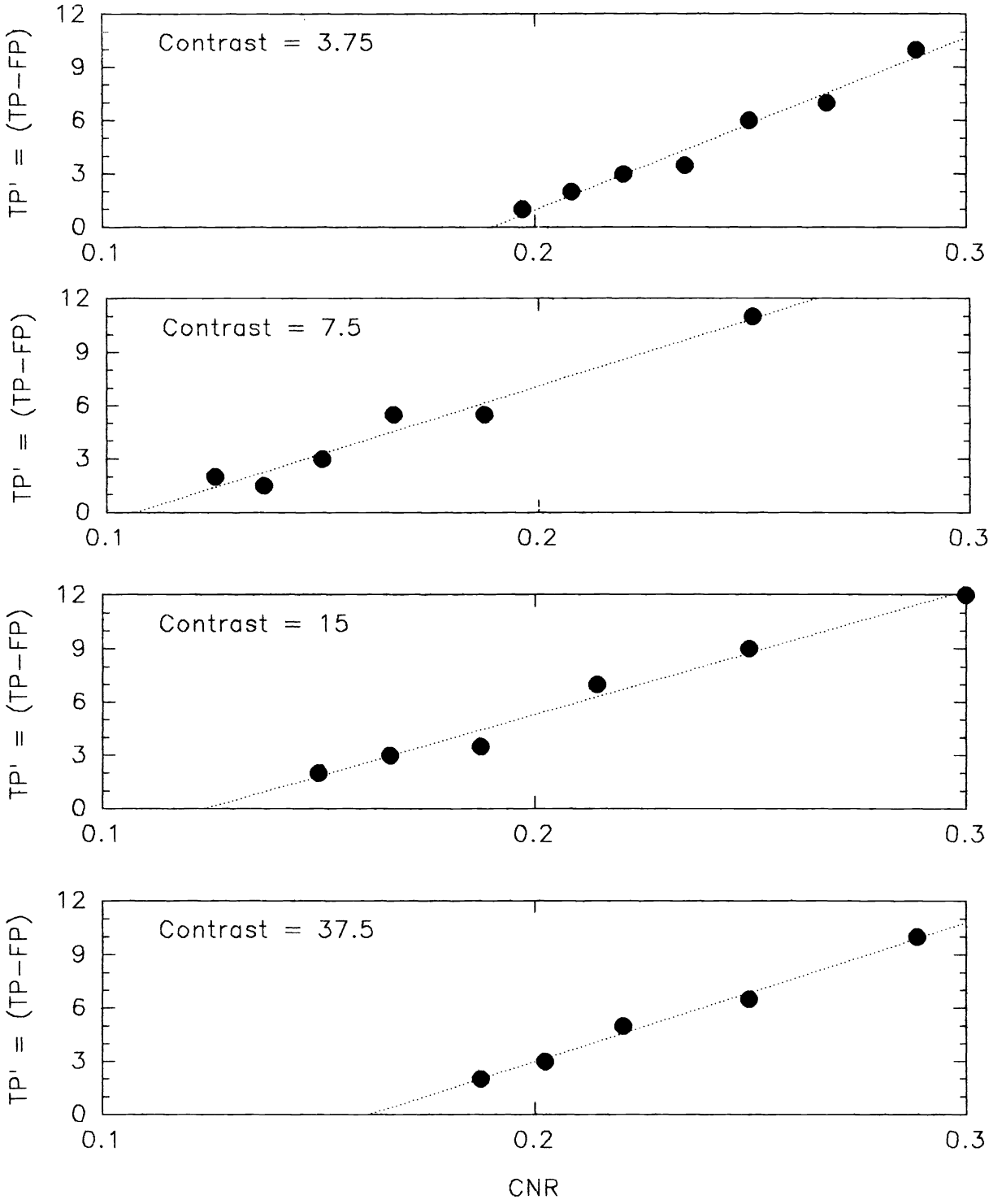

Figure 2

Effective sensitivity vs Contrast to Noise ratio

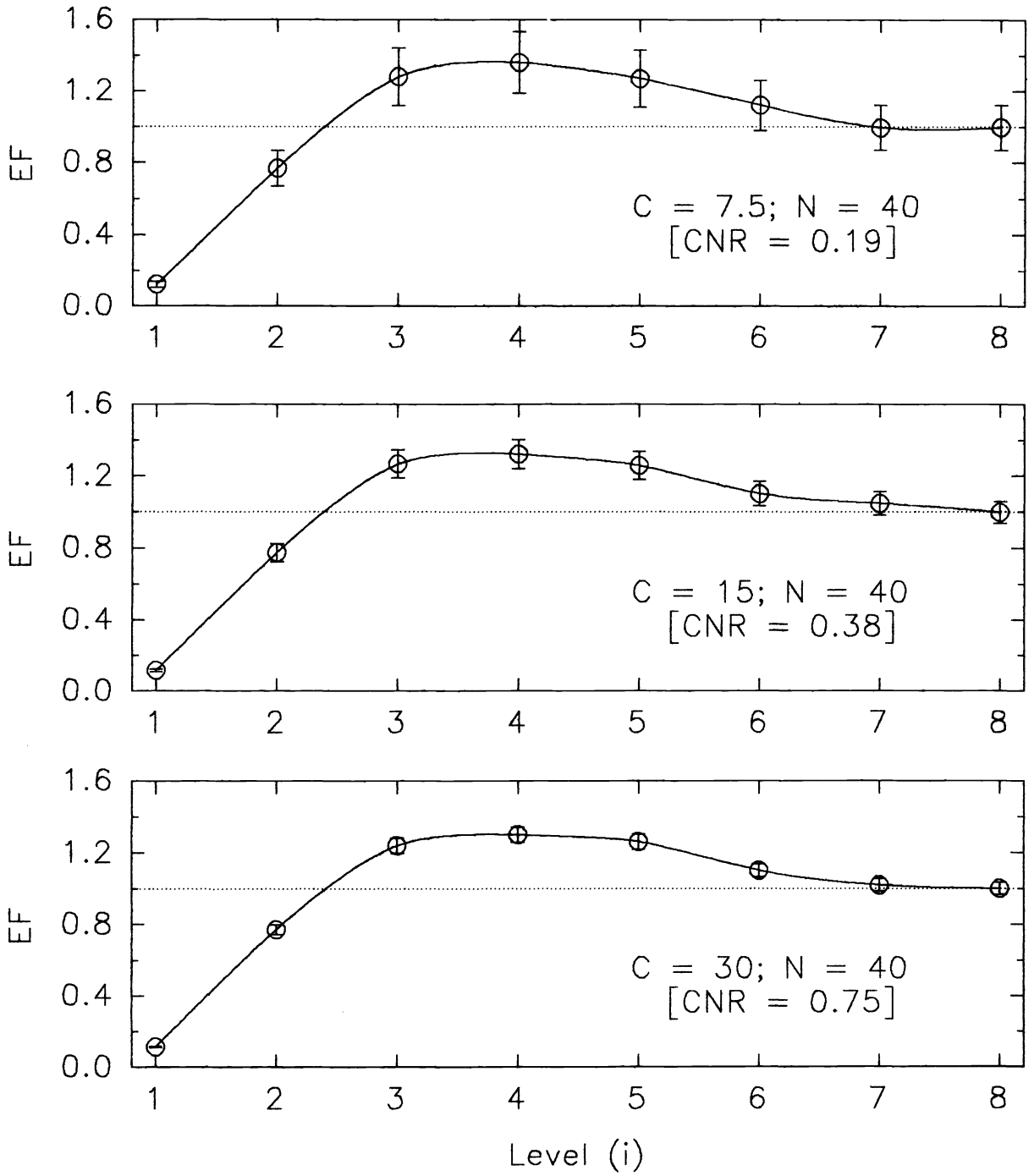

Figure 3

Enhancement factor vs level (i)

[Gain 20; Threshold 2.5]

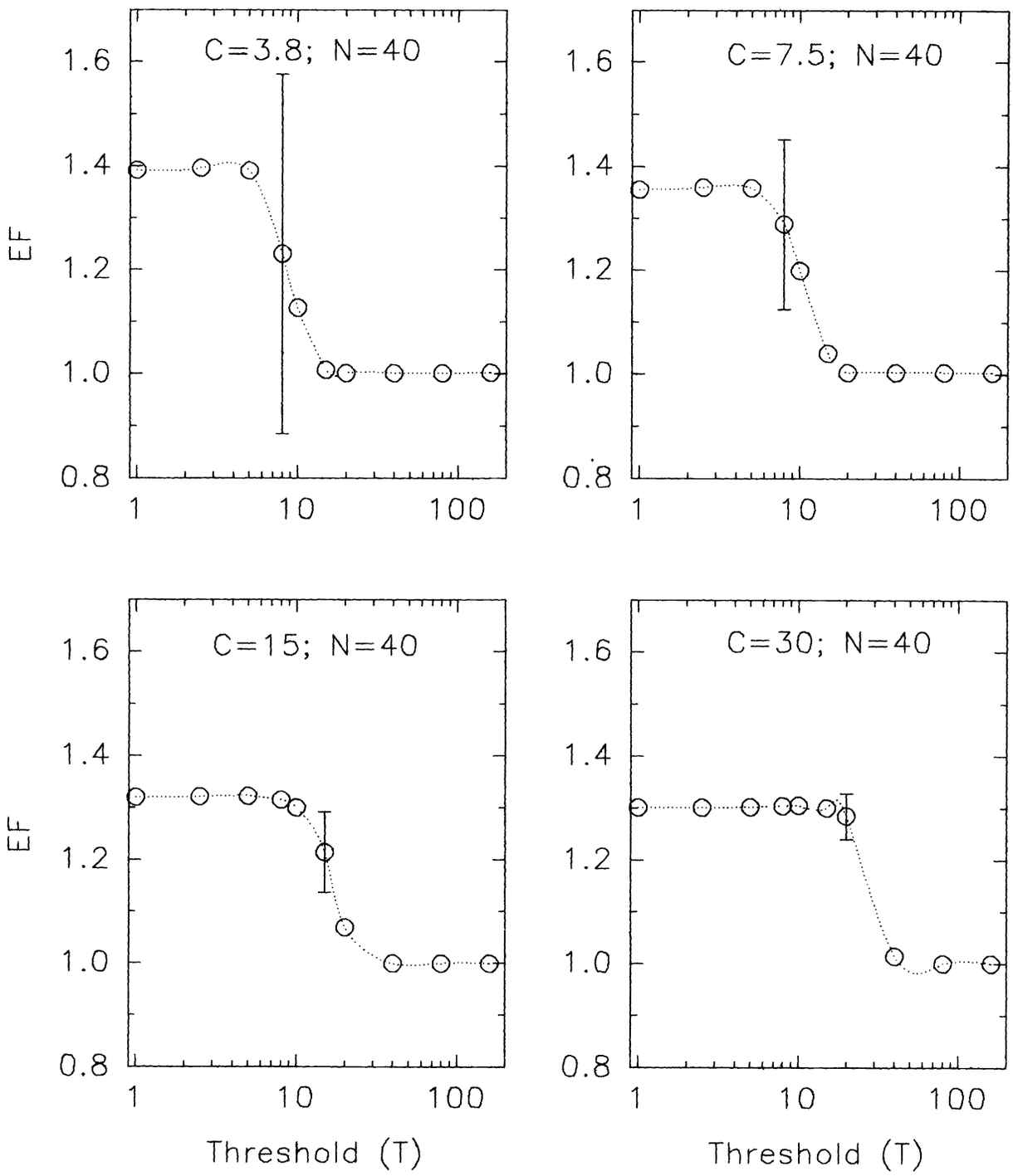

Figure 4
Enhancement factor vs threshold
[Gain 20; Level i = 4]

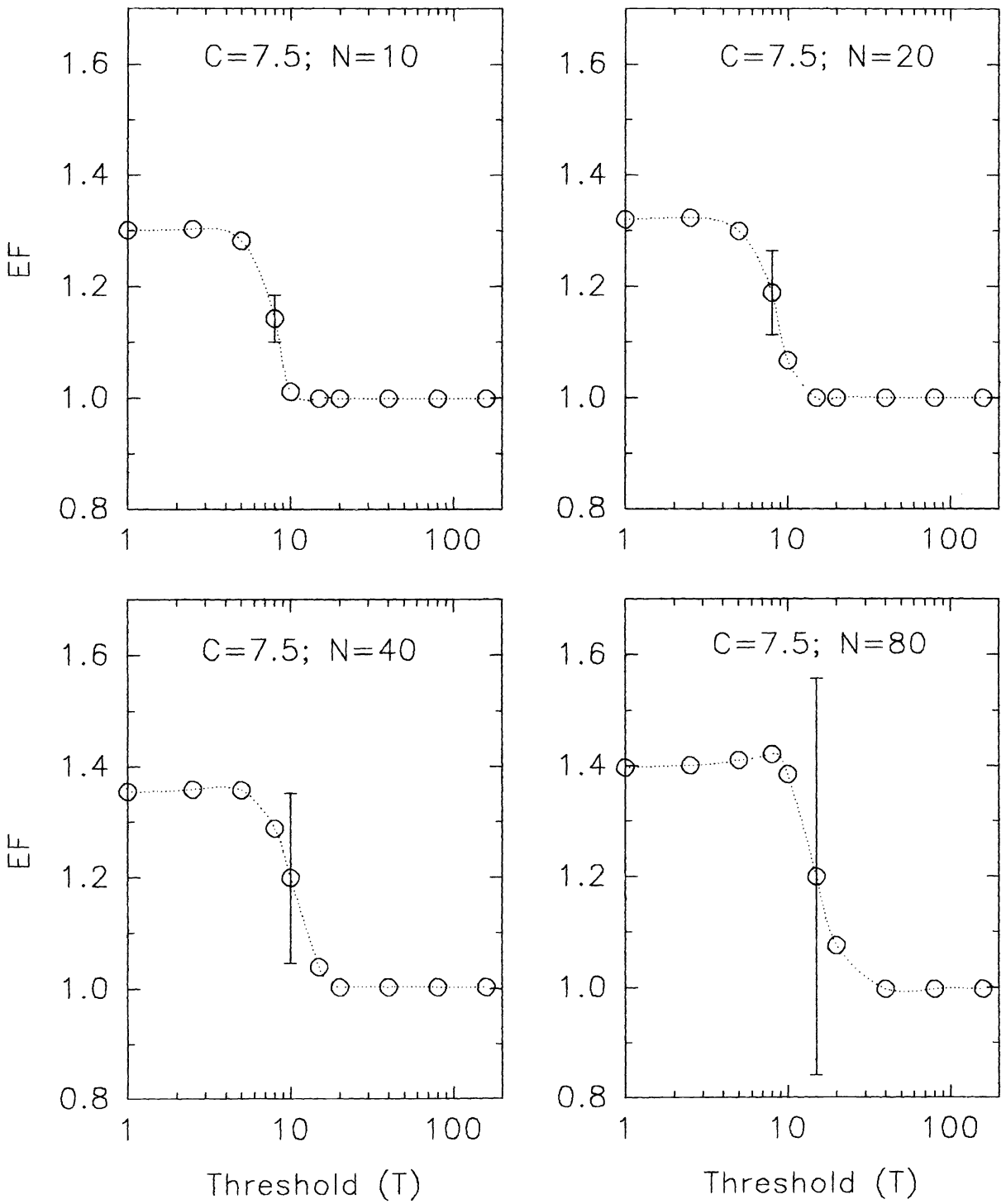

Figure 5

Enhancement factor vs threshold

[Gain 20; Level i = 4]

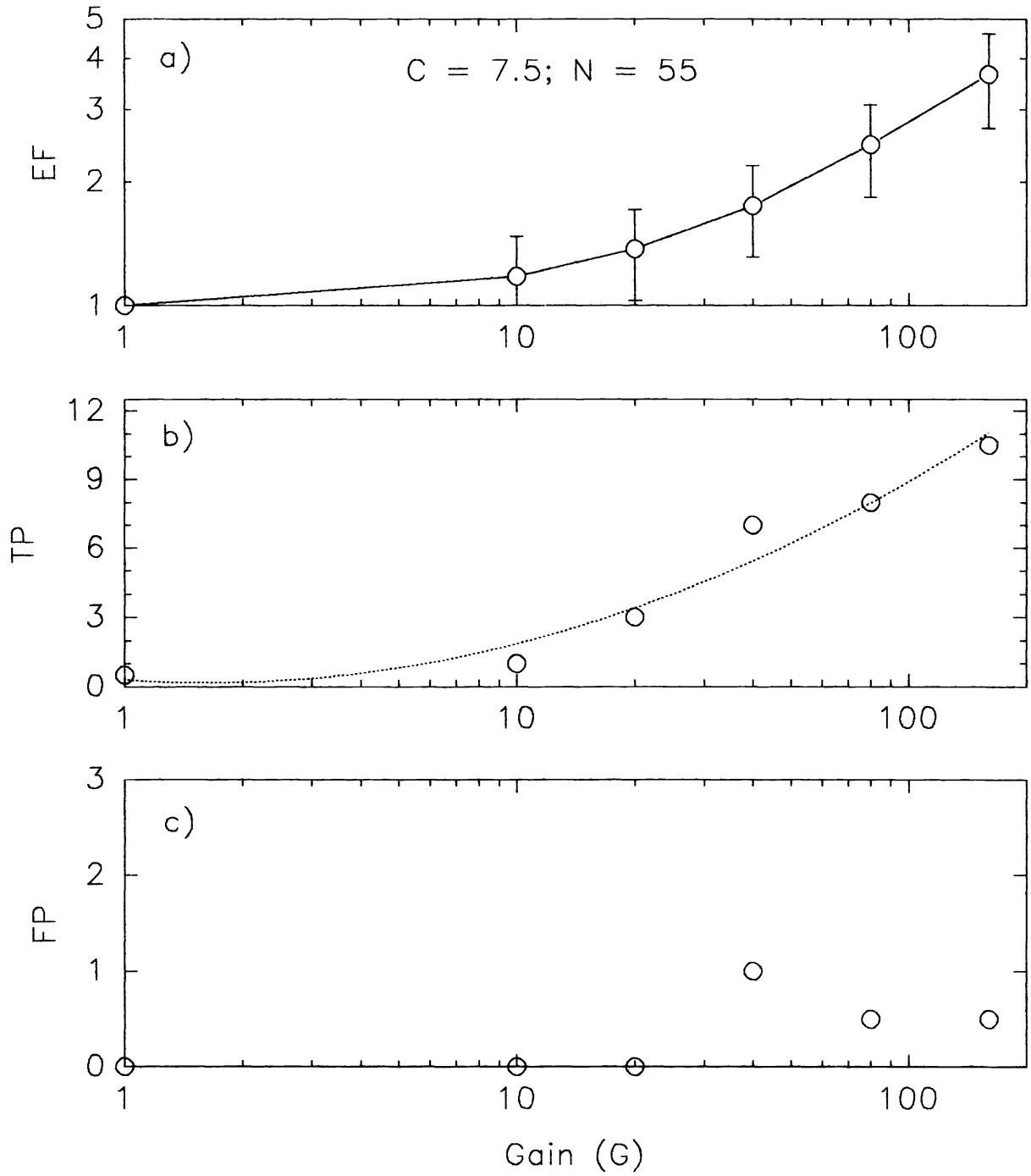

Figure 6

a) EF vs Gain; b) TP vs Gain; c) FP vs Gain

[Level i = 4; Threshold 0.25]